Copolymers under a Monomer Orienting Field

Eugene Gurovich*

Groupe de Physico-Chimie Theorique, ESPCI, 75231 Paris Cedex 05, France

Received March 22, 1994; Revised Manuscript Received August 19, 1994®

ABSTRACT: A microscopic statistical theory of diblock copolymer melts in an electric field is developed within the framework of the random phase approximation. We predict that near the spinodal point copolymer melts reveal four different universal types of behavior. In determining to which universal class the copolymer melt belongs, the only relevant parameters turn out to be f, the fraction of monomers A in a chain, and parameters $S^{(A)}$ and $S^{(B)}$, which characterize how many times the radii of gyration of blocks A and B increase, respectively, along an applied field during birefringence. The theory explains and gives quantitative results for the alignment of ordered structures and for the shift of transition temperatures.

Introduction. Recent experimental developments in electric-field-induced and deformation-induced phenomena in polymer solutions, blends, and copolymer melts have opened new options for their industrial applications, which are hard to overestimate.

Moriya et al.[1] were the first to demonstrate that an electric field generates anisotropic structures in blends, and suggested a new approach for the modulation of blend morphology. Recently Venugopal et al.[2] observed in blends a strange slanting of "pearl chains" with respect to the applied field. The effect of the field on diblock copolymers was recently discussed by Amundson et al.[3] They reported on a macroscopic alignment of a lamellar microstructure while cooling through the order–disorder transition (electric-field-induced orientation). Moreover, small angle X-ray scattering (SAXS) results clearly showed the persistence of an ordered structure even after heating the materials 14 K above the critical temperature given for zero electric field (electric-field-induced shift of the microphase separation). The electric-field-induced remixing in the two-phase region for binary polymer solutions was observed and discussed by Wirtz et al.[4]

A large body of data has been accumulated on the fascinating behavior of copolymers under deformations. These experiments were pioneered 20 years ago by Keller et al.,[5] who performed various investigations by melting and stretching triblock copolymers. Deformation-induced orientation phenomena were discovered: the treatment altered and reformed lamellar and honeycomb-like patterns, the hexagonal axis always being consistent with the direction of the extrusion. Deformation-induced shift of the microphase separation transition in triblocks was reported, for the first time, probably, by Terrisse,[6] who had shown that the oscillatory shearing above a certain frequency destroys the long-range order. Hadziioannou et al.[7] found that diblocks as well as triblock are reformed by shear: axes of hexagonally packed cylinders are aligned with the direction of the shear, and the lamellar phase is arranged parallel to the plane of the shear. SAXS results, important for the understanding of field induced phenomena, were recently presented by Morrison et al.[8] They have shown how the sphere of critical wave vectors (defined in the reciprocal space) is split into more complicated forms under increasing shear. And, recently Koppi et al.[9] confirmed the deformation-driven lamellar phase orientation and the shift of the order–disorder transition temperature and discovered a reorientational phase transition: near the spinodal point the change in the frequency of shear transforms lamellar oriented parallel to the flow into lamellar oriented perpendicular to it. Balsara and Hammouda[10] reported on deformation-induced orientation in solvated diblocks and Romo-Uribe and Windle[11] studied the reorientational phase transition in random copolymers.

A probable suppression by deformations and electric fields of the body-centered-cubic phase, as yet unobserved, completes a renumeration of the principal phenomena induced by fields, phenomena which are amusingly reproducible in different complex polymeric melts.

In this paper, we report results[12] of a microscopic mean-field theory of microphase separation for diblocks in an applied electric field. The main point of the current theory is that, in the presence of a monomer orienting field, it is not the simple composition f, but rather a more complicated object, an effective composition, describes the configurational entropy of chains and is a relevant parameter of the problem.

Diblocks are exceptionally well-suited for experimental investigations. The are also a very good model system for understanding the general features of microphase formation and organization in complex fluids under external fields. The phase behavior of these systems has been described in terms of a few molecular parameters such as the polymerization degrees of the blocks N_A and N_B and the Flory-Huggins parameter χ, which characterizes the effective interaction between incompatible A and B monomers. The emerging thermodynamic picture of microphase separation (based on the random phase approximation) seems to be quite satisfactory.

The random phase approximation for microseparation of diblocks was developed by Leibler.[13] The essential result is that the only relevant parameters for phase behavior turn out to be the product χN and f, the fraction of A statistical segments in a chain. For Gaussian chains the composition f can be represented as follows:

$$\frac{f}{1-f} = \frac{(R^{(A)})^2}{(R^{(B)})^2} \tag{1}$$

where $R^{(A)}$ and $R^{(B)}$ are gyration radii of ideal A and B blocks

$$(R^{(A)})^2 = \frac{N_A a^2}{6}$$

$$(R^{(B)})^2 = \frac{N_B a^2}{6}$$

respectively, and a is the statistical segment length.

---

* Present address: The Department of Physics, The Institute of Theoretical Physics, Technion, 3200 Haifa, Israel.

® Abstract published in *Advance ACS Abstracts*, October 15, 1994.

0024-9297/94/2227-7063$04.50/0

As χN is increased, a competition between the repulsive energy of incompatible links and the configurational entropy produces the microphase separation. At the spinodal the diblock melt becomes absolutely unstable: composition fluctuations with critical wave vectors diverge. In the reciprocal space the critical wave vectors form a sphere. In reality, the weak first-order transitions (disordered melt → lamellar → hexagonal → body-centered-cubic lattices) forestall the spinodal decomposition.

Electric Field Birefringence. For nonrandomly oriented segments, chains are not Gaussians. For instance, electric field $\vec{E}$ polarizes monomers, interacts with induced polar moments, and orients them. It gives rise to birefringence phenomena.[14] For positive anisotropic polarizability of monomers, chains are elongated parallel to an applied field, $\vec{E}$, and by contrast, for negative anisotropic polarizabilities, chains are compressed along $\vec{E}$. The squared gyration radii of ideal A and B blocks parallel and perpendicular to an applied electric field, R_l and R_p, are

$$(R_l^{(i)})^2 = (R^{(i)})^2 S^{(i)}$$

$$2(R_p^{(i)})^2 = (R^{(i)})^2 (3 - S^{(i)}) \tag{2}$$

Here $S^{(i)}$ is a parameter which characterizes the elongation of a block (i = A, B) by the electric field and depends on the temperature, the electric field intensity, and the anisotropic polarizability of a segment. The physical meaning of S is clear: $S = 3\langle cos^2\,\theta\rangle$, where θ is the angle between the applied field and the statistical segment.

Effective Composition of a Diblock in an Electric Field. In the absence of an electric field, the entropy of an ordered chain depends upon the composition f. For Gaussian chains, the composition f is defined as the ratio of A block statistical segments (N_A) to the full number ($N_A + N_B$) of statistical segments.

If the anisotropic polarizabilities of A and B monomers are the same, the chain blocks will be elongated (compressed) by applied field in the same way. In such a case, compositions defined through the statistical segments associated with gyration radii of blocks along and perpendicular to the electric field are also the same,

$$\frac{f}{1-f} = \frac{(R_l^{(A)})^2}{(R_l^{(B)})^2} = \frac{(R_p^{(A)})^2}{(R_p^{(B)})^2} \tag{3}$$

and coincide with the composition f defined for zero electric field.

In general, blocks are deformed differently by an applied field. The stiffness of a chain depends on its local orientation with respect to the electric field. As a result, the composition of a copolymer related with the conformational properties of a diblock cannot be defined unambiguously. For instance, effective compositions associated with the statistical segments measured along the perpendicular to the electric field, f_*^* and f_*^{**}, are different:

$$\frac{f_*^{**}}{1-f_*^{**}} = \frac{(R_p^{(A)})^2}{(R_p^{(B)})^2} = \frac{f(3-S^{(A)})}{(1-f)(3-S^{(B)})}$$

and

$$\frac{f_*^*}{1-f_*^*} = \frac{(R_l^{(A)})^2}{(R_l^{(B)})^2} = \frac{fS^{(A)}}{(1-f)S^{(B)}} \tag{4}$$

Since the configurational entropy of a diblock depends on the numbers of the A and B statistical segments, one concludes that in the presence of an external field, it is not the simple composition f, but rather a more complicated object, an effective composition, is a relevant parameter for phase behavior.

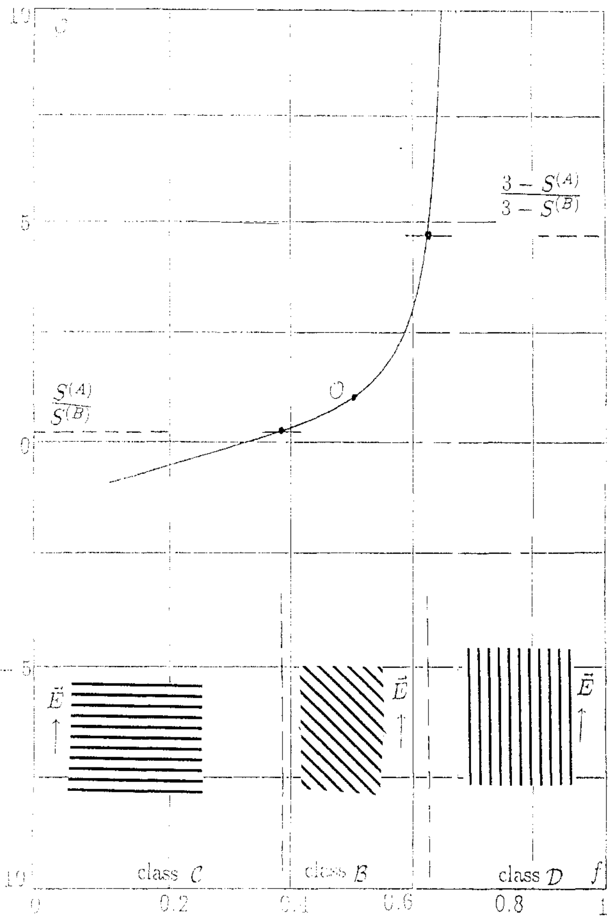

Figure 1. The diagram of universal classes for diblocks. The universal function $\mathcal{G}$ depends solely on the composition f. It equals zero and infinity at f = 0.331 and 0.669, respectively. These numbers limit the composition region for class $\mathcal{B}$.

Critical Wave Vectors. Four Universal Classes. In isotropic diblock melts, critical wave vectors form a sphere; i.e., at the spinodal point, fluctuations of the concentration with critical wave vectors of some fixed length, $|\vec{Q}| = Q^*$, diverge. An applied field breaks this isotropic (spherical) symmetry. A detailed analysis shows that in dependence of three parameters, f, $S^{(A)}$, and $S^{(B)}$, critical wave vectors can form an axial ellipsoid (class $\mathcal{A}$), one (class $\mathcal{D}$) or two (class $\mathcal{B}$) rings perpendicular to the field, and two points parallel to the field (class $\mathcal{C}$). Classes $\mathcal{B}$, $\mathcal{C}$, $\mathcal{D}$ and transitions between them are conveniently presented in a universal class diagram (Figure 1). The function $\mathcal{G}$ depends only on the composition f and on the copolymer architecture. Two values of the composition f for which the universal function $\mathcal{G}(f)$ equals

$$\frac{3-S^{(A)}}{3-S^{(B)}}$$

and

$$\frac{S^{(A)}}{S^{(B)}}$$

divide the whole composition region into three classes $\mathcal{B}$, $\mathcal{C}(\mathcal{D})$, and $\mathcal{D}(\mathcal{C})$, as it is shown in Figure 1. Neither the Flory-Huggins parameter, χ, nor the degree of polymerization, N, will change the class of the copolymer melt. Each class has its specific X-ray diffraction pattern near

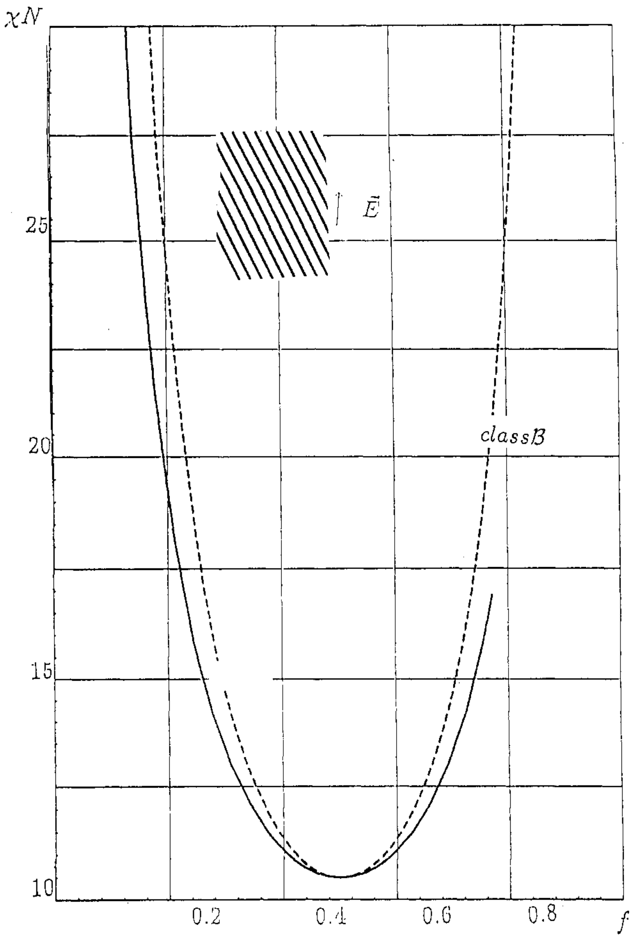

Figure 2. The spinodal line for a copolymer melt of class $\mathcal{B}$ vs the composition f. It does not depend on the electric field intensity and is always smaller than the spinodal (the dashed line) for zero electric field.

the spinodal point, its specific dependence of the order–disorder transition temperature on the applied field, and its specific cascade of phase transitions under microphase separation.

Class $\mathcal{A}$ represents strongly degenerate-in-electric-field copolymers, for which the anisotropic parts of the A and B monomer polarizabilities are equal. Since this situation is hardly experimentally realizable, I will not discuss class $\mathcal{A}$ in the paper.

For class $\mathcal{B}$, critical fluctuations are concentrated in Q-space on two rings perpendicular to the electric field. A second-order transition from a disordered to a tilted lamellar phase coincides for any composition f with the spinodal (Figure 2). The transition temperature does not depend on the intensity of the applied field. Given composition f and an applied field E, the angle between the field and the direction along which the microphase separation pattern appears depends on the electric field intensity. The squared tangence between the normal to lamellar layers and the applied electric field is

$$\frac{1}{2}\frac{(3 - S^{(B)})\mathcal{G}(f) - (3 - S^{(A)})}{S^{(A)} - S^{(B)}\mathcal{G}(f)}$$

where the function $\mathcal{G}(f)$ is shown in Figure 1. The lamellar phase for class $\mathcal{B}$ is, in fact, smectic C.

For class $\mathcal{C}$, only fluctuations with wave vectors oriented strictly along the electric field diverge at the spinodal point, and critical fluctuations are concentrated in Q-space on two points. For any composition, f, the lamellar phase oriented perpendicularly to the electric field appears by a second-order transition from a homogeneous melt. The effective composition f^*_*, associated with the statistical segment length along the field, seems to be a more relevant parameter than the composition f. The spinodal line and pattern periodicity (as functions of f^*_*) depend on the intensity of the electric field. The values of χN for a disordered melt → lamellar phase transition are shifted by the electric field to smaller values of χN in comparison with those calculated for a zero electric field.

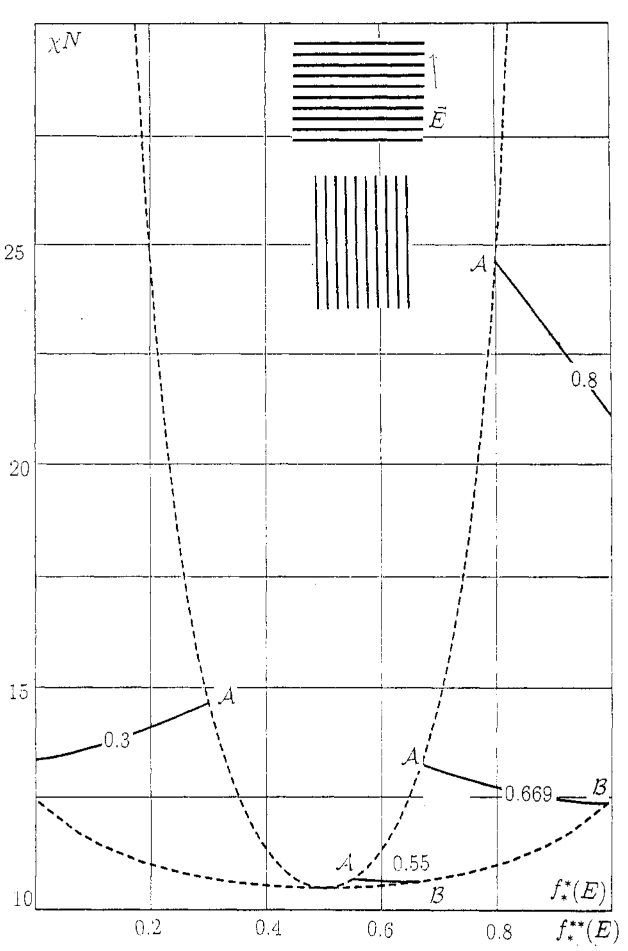

Figure 3. The spinodal lines for a copolymer melt of class $\mathcal{C}(\mathcal{D})$ vs f^*_* ($\tilde{f}^{**}_*$), for $f = 0.3, 0.55, 0.669$, and 0.8. The dashed line is the spinodal vs f for zero electric field.

For class $\mathcal{D}$, the critical wave vectors form a ring perpendicular to the electric field. For any composition f, while increasing χN, two-dimensional honeycomb and lamellar phases oriented strictly parallel to the electric field appear by first-order transitions. The effective composition f^{**}_*, associated with the statistical segment length perpendicular to the field, is a more relevant parameter than the composition f. The spinodal line (Figure 3) and the pattern periodicity as a function of the effective composition f^{**}_* depend on the electric field intensity and are the same as for class $\mathcal{C}$.

Increasing the electric field leads to transitions between different classes. For instance, the lamellar phase oriented perpendicularly to the electric field should be spontaneously transformed [by orientational phase transitions smectic A (class $\mathcal{C}$) → smectic C (class $\mathcal{B}$) → smectic A (class $\mathcal{D}$)] into lamellar oriented parallel to the field.

All these mean-field effects described and predicted above should be observable for symmetric diblock copolymers to provide a detailed verification of the theory. Unfortunately, until now, systematic experimental studies of molten copolymers under strong electric fields were not available. On the other hand, predicted by us phenomena, such as the distinct types of behavior, the splitting of sphere of the critical wave vectors, the shift of transition temperatures and spinodal lines, the suppression of the body-centered-cubic phase, and the induced orientational and reorientational transitions, make direct contacts with a variety of experiments on dynamical behavior of copolymers, the comprehensive theory of which is in preparation.

Acknowledgment. Support for the research was provided by the Elf-Aquitaine Company and CNRS. This work was performed during my stay at the Laboratoire de Physico-Chimie Theorique, ESPCI, in Paris. I am very grateful to Ludwik Leibler and Jacques Prost. The present work as the focus of research was clarified and inspired by enlightening discussions with them.

References and Notes

(1) Moriya, S.; Adachi, K.; Kotaka, T. *Polym. Commun.* **1985**, *26*, 235.
(2) Venugopal, G.; Krause, S.; Wnek, G. E. *J. Polym. Sci., Part C: Polym. Lett.* **1989**, *27*, 497; *Polym. Prepr.* (*Am. Chem. Soc., Div. Polym. Chem.*) **1990**, *31* (1), 377. Serpico, P.; Wnek, G. E.; Krause, S.; Smith, T. W.; Luca, D. J.; Van Laeken, A. *Macromolecules* **1992**, *25*, 6373.
(3) Amundson, K.; Helfand, E.; Patel, S. S.; Quan, X. *Macromolecules* **1991**, *24*, 6546.
(4) Wirtz, D.; Berend, K.; Fuller, G. G. *Macromolecules* **1992**, *25*, 7234.
(5) Keller, A.; Pedemonte, E.; Willmouth, F. M. *Nature* **1970**, *225*, 538.
(6) Terrisse, J. Thesis of Universite Louis Pasteur de Strasburg, 1973.
(7) Hadziioannou, G.; Picot, C.; Skoulios, A.; Ionescu, M. L.; Mathis, A.; Duplessix, R.; Gallot, Y.; Lingelser, J. P. *Macromolecules* **1982**, *15*, 263.
(8) Morrison, F.; Winter, H.; Gronski, W.; Barnes, J. D. *Macromolecules* **1990**, *23*, 4200; Morrison, F., Winter, H. *Macromolecules* **1989**, *22*, 3533.
(9) Koppi, K. A.; Tirrell, M.; Bates, F. S.; Almdal, K.; Colby, R. H. *J. Phys. 2* **1992**, *2*, 1941.
(10) Balsara, P. N.; Hammouda, B. *Phys. Rev. Lett.* **1994**, *72*, 360.
(11) Romo-Uribe A.; Windle, A. H. *Macromolecules* **1993**, *26*, 7100.
(12) Gurovich, E., submitted to *Macromolecules*, **1994**.
(13) Leibler, L. *Macromolecules* **1980**, *13*, 1602.
(14) Kuhn, W. *Kolloid Z* **1934**, 68, 2; *J. Polym. Sci.* **1946**, *1*, 360.